JOURNAL OF GEOPHYSICAL RESEARCH, VOL. 99, NO. B1, PAGES 531–541, JANUARY 10, 1994

Variations in ridge morphology and depth-age relationships on the Pacific-Antarctic ridge

Karen M. Marks

Geosciences Laboratory, Ocean and Earth Sciences, National Ocean Service, NOAA, Silver Spring, Maryland

Joann M. Stock

Seismological Laboratory, California Institute of Technology, Pasadena

Abstract. Adjacent segments of the Pacific-Antarctic ridge display significantly different morphologies and depth-age relationships over seafloor younger than 36 Ma. The spreading corridor southwest of Fracture Zone XII is characterized by a rift valley and an usually small subsidence constant of 226 ± 13 m/m.y.$^{1/2}$, while the two spreading corridors immediately northeast of Fracture Zone XII have an axial high and a subsidence constant consistent with the global average. This abrupt variation in ridge morphology is not usually characteristic of medium-rate spreading centers, nor is such an abrupt variation expected of adjacent ridge segments that are spreading at the same rate. We suggest that a thermal anomaly beneath the ridge may influence the first-order effects of spreading rate and lithospheric cooling enough to produce the observed rift valley and axial high and the different subsidence constants. Although we are not certain what would produce the thermal anomaly here, we speculate that when the spreading rate on the Pacific-Antarctic ridge increased from slow to intermediate rates since 20 Ma, so did the need for materials for accretion, which may be supplied in part by along-axis asthenospheric flow from hotspots or a hot region to the northeast. A sufficient supply of hot asthenosphere may still be lacking in the ridge segment with the axial valley to the southwest, leaving it cooler and starved for accretionary materials.

Introduction

It is well known that the depth of the ocean floor increases with age and distance from the spreading ridge. This occurs because oceanic lithosphere cools and contracts as it moves away from the ridge. As the plate cools, the isotherms deepen, and cooling upper mantle rocks underplate and thicken the lithosphere. The lithosphere therefore becomes denser and thicker with age, and it subsides isostatically [*Turcotte and Schubert*, 1982].

Two types of thermal models have been used to predict the relationship between the depth of the seafloor and its age: the cooling plate model [*McKenzie*, 1967], and the thermal boundary layer (or cooling half-space) model [*Turcotte and Oxburgh*, 1969]. Both models predict a linear increase in depth with the square root of age for seafloor younger than about 60 Ma. For older seafloor the depth continues to increase in the thermal boundary layer model, while it approaches a constant value for the cooling plate model. Since the seafloor in our study area is younger than 60 Ma, either model could theoretically explain the observed depth-age relationship with an equation of the following form:

$$\text{depth} = d_0 + C(\text{age}^{1/2})$$

where d_0 is the ridge crest depth and C, the subsidence constant, is

$$C = \frac{2\rho_m \alpha T_m}{\rho_m - \rho_w}\left(\frac{\kappa}{\pi}\right)^{1/2}$$

The subsidence constant depends on the thermal parameters T_m, the temperature of the asthenosphere; κ, the thermal diffusivity; and α, the coefficient of thermal expansion; as well as ρ_m and ρ_w, the density of mantle and water, respectively. When the subsidence constant is determined from observations, these parameters represent the average thermal regime over the range of ages used.

Several researchers have attempted to determine values for d_0 and C empirically. For example, *Parsons and Sclater* [1977] found that a ridge crest depth of 2500 m and subsidence constant of 350 m/m.y.$^{1/2}$ best described data from the North Atlantic and North Pacific oceans, and for many years these values have been adopted as the global average. *Cochran* [1986] showed that the best fit subsidence constant at least for the Southeast Indian and South Pacific oceans lies within the range 340–390 m/m.y.$^{1/2}$. More recently, it has been recognized that d_0 and C may vary regionally from ocean to ocean [*Hayes*, 1988; *Marty and Cazenave*, 1989] or locally along a length of ridge [*Cochran*, 1986; *Hayes*, 1988] or even from one side of a spreading center to the other so that the flanks are subsiding asymmetrically [*Hayes*, 1988]. On the basis of global compilations of depth and heat flow data, various revisions to *Parsons and Sclater*'s [1977] empirical constants have been proposed: d_0 = 2600 m, C = 365 m/m.y.$^{1/2}$ for ages <20 Ma [*Stein and Stein*, 1992]; and d_0 = 2700 m, C = 300 m/m.y.$^{1/2}$ for ages <60 Ma [*Hayes*, 1988].

Paper number 93JB02760.
0148-0227/94/93JB-02760$05.00

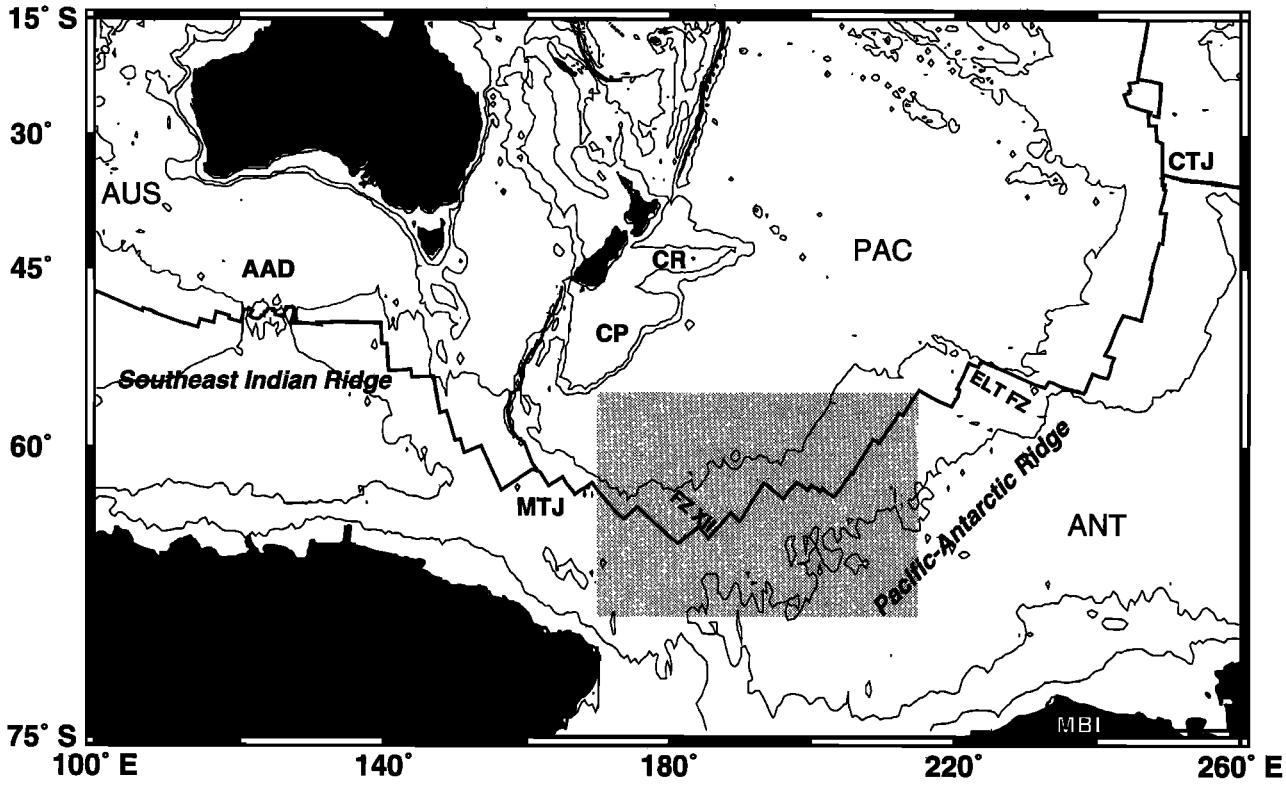

Figure 1. Location of study area (shaded region). Thin lines are ETOPO5 bathymetric contours (contour interval is 2000 m), heavy lines are plate boundaries between the Pacific (PAC), Antarctic (ANT), and Australian (AUS) plates. The Macquarie triple junction (MTJ), Chile triple junction (CTJ), Australian-Antarctic discordance (AAD), Campbell plateau (CP), Chatham rise (CR), and Marie Byrd Land (MBL) are referred to in the text.

It is also recognized that the morphology of ridges depends on spreading rate. Slow spreading ridges (10–50 mm/yr) are typically associated with a prominent rift valley and rough topography, intermediate rate spreading ridges (50–90 mm/yr) with a small median valley (50–200 m deep) and subdued topography, and fast spreading ridges (>90 mm/yr) with smooth topography and an axial high (no rift valley) [*Macdonald*, 1982, 1986]. Exceptions to this pattern occur in the vicinity of hotspots, where slow and intermediate rate spreading ridges may exhibit axial morphology typical of fast spreading ridges, due perhaps to elevated mantle temperatures and excess melt [*Cochran*, 1986; *Chen and Morgan*, 1990]. Ridge morphology may change abruptly across transform faults [*Cochran*, 1986; *Hayes*, 1988; *Marks et al.*, 1990; *Small and Sandwell*, 1992], but this abrupt change is not always simply related to spreading rate [*Cochran*, 1991].

Here we examine the morphology and depth-age relationships of adjacent spreading corridors on the Pacific-Antarctic ridge. The observed differences in ridge morphology and subsidence constants cannot be simply explained by first-order models of spreading rate and lithospheric cooling. This suggests that some other process dominates the ridge morphology and influences the subsidence rates of this portion of the Pacific-Antarctic ridge. We compare these observations of the Pacific-Antarctic ridge to another spreading ridge that displays similar features, and explore the process(es) that may produce them.

Tectonic Setting

The Pacific-Antarctic spreading center separates the Pacific and Antarctic plates, between the Macquarie triple junction (~160°E, 62°S) and the Chile Triple Junction (~250°E, 35°S) (Figure 1). It has been an active spreading center since Late Cretaceous time, when seafloor spreading rifted the Campbell plateau and the Chatham rise (Pacific plate) apart from Marie Byrd Land (Antarctic plate). However, its ridge segments and transform faults and its spreading rates have evolved considerably since the time of the first recorded magnetic anomalies there (chron 34, 84 Ma [*Kent and Gradstein*, 1985]), due to plate reorganizations in the south Pacific [e.g., *Molnar et al.*, 1975; *Cande et al.*, 1982; *Mayes et al.*, 1990]. These major changes in relative plate motions have been recorded in the magnetic anomalies of the seafloor, and also in the sinuosity of the fracture zones generated at this spreading center. Slower spreading in the past is indicated in the ship magnetics and by the rough seafloor that is pervasive along both flanks of the Pacific-Antarctic ridge. *Mayes et al.* [1990] determined that the spreading rate of the Pacific-Antarctic ridge increased from 42 to 56 mm/yr about 10 m.y. ago and reached its present-day rate of ~60–65 mm/yr about 4.7 m.y. ago.

Detailed ship surveys have been conducted over the Eltanin fracture zone system at the northern end of the spreading center [*Lonsdale*, 1986] and over a transform fault and fracture zone (Fracture Zone XII (FZ XII)) at the

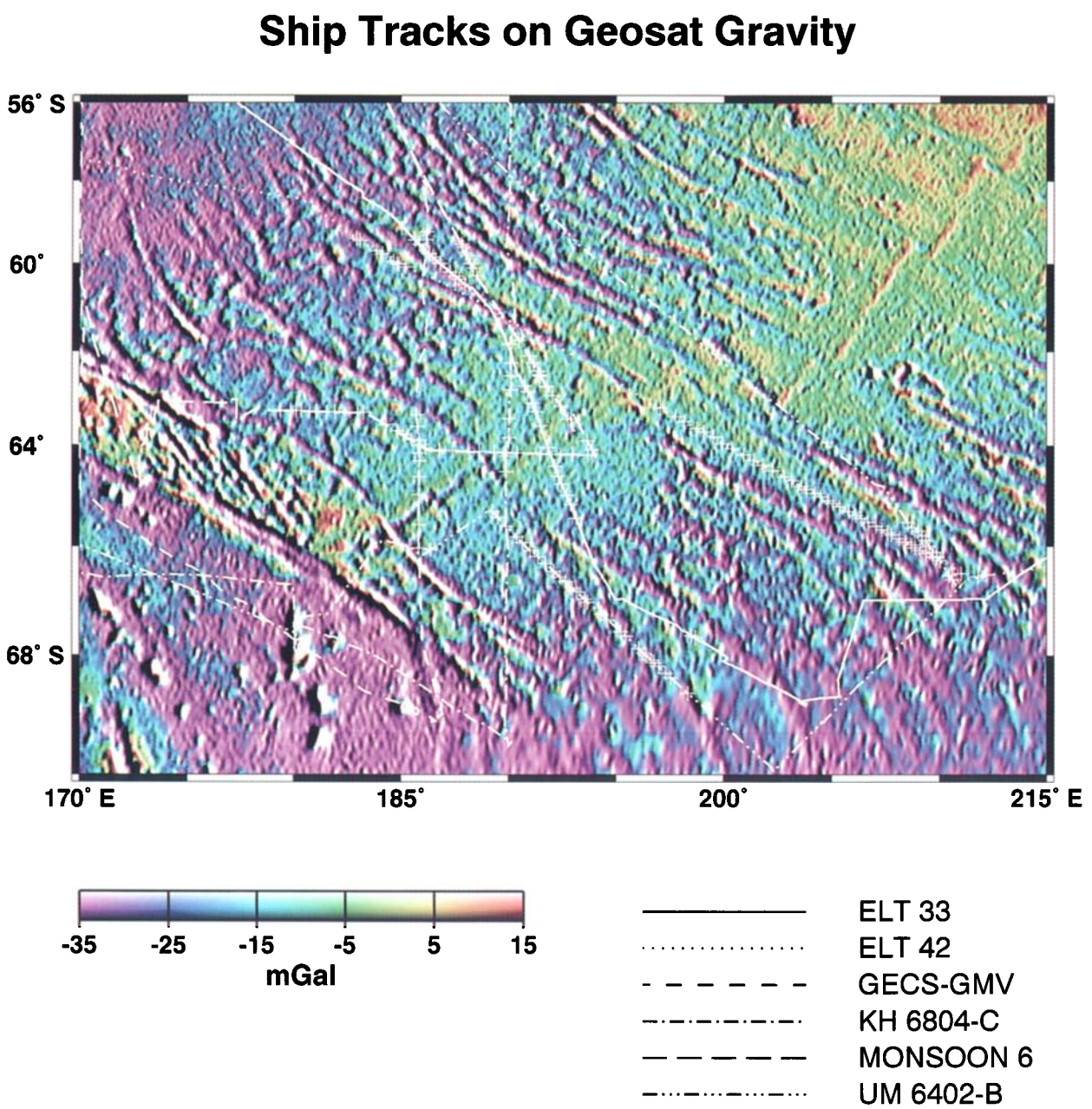

Plate 1. Geosat gravity field over the Pacific-Antarctic ridge study area. Gravity anomaly amplitudes range between ≤ -35 mGal (magenta) and $\geq +15$ mGal (red) and are "illuminated" from the east. Ship tracks are heavy white lines; magnetic anomaly locations are marked with pluses.

southwestern end of the ridge [*Cande et al.*, 1992; *Haxby et al.*, 1992]. However, between these two areas, the Pacific-Antarctic spreading center is only sparsely surveyed by ships. There are large regions of seafloor (>10,000 km^2) lacking shipboard magnetic, gravity, or bathymetry observations. As a result, most of the fracture zones that trace the plate motions of the southwest Pacific are very poorly defined by ship bathymetry (for example, see GEBCO charts covering the Pacific-Antarctic ridge [*Canadian Hydrographic Service*, 1982]), and there are large areas of seafloor that have no magnetic anomaly identifications [e.g., *Cande et al.*, 1989]. Moreover, until the recent declassification of the Geosat Geodetic Mission (GM) data south of 30°S, even major tectonic features of the seafloor (such as a small-offset ridge/transform system that originated as a leaky transform fault about 4.7 m.y. ago) remained undiscovered [*Marks et al.*, 1991a].

Because short-wavelength gravity anomalies (<400 km) are highly correlated with small-scale seafloor topography, we are able to use the high resolution gravity fields computed from Geosat GM and ERM data [*Marks et al.*, 1993b] to map the tectonic features of the seafloor beneath the Southern Ocean [*McAdoo and Marks*, 1992; *Marks et al.*, 1993a]. In Plate 1 we show the high-resolution gravity anomalies covering our selected study area on the Pacific-Antarctic ridge. These anomalies reveal fine-scale features such as a southwesterly pointing propagating rift located on the ridge axis at 195°E, a portion of the small-offset ridge/transform system that connects the Southeast Indian ridge to the southernmost segment of the Pacific-Antarctic ridge and irregular traces in

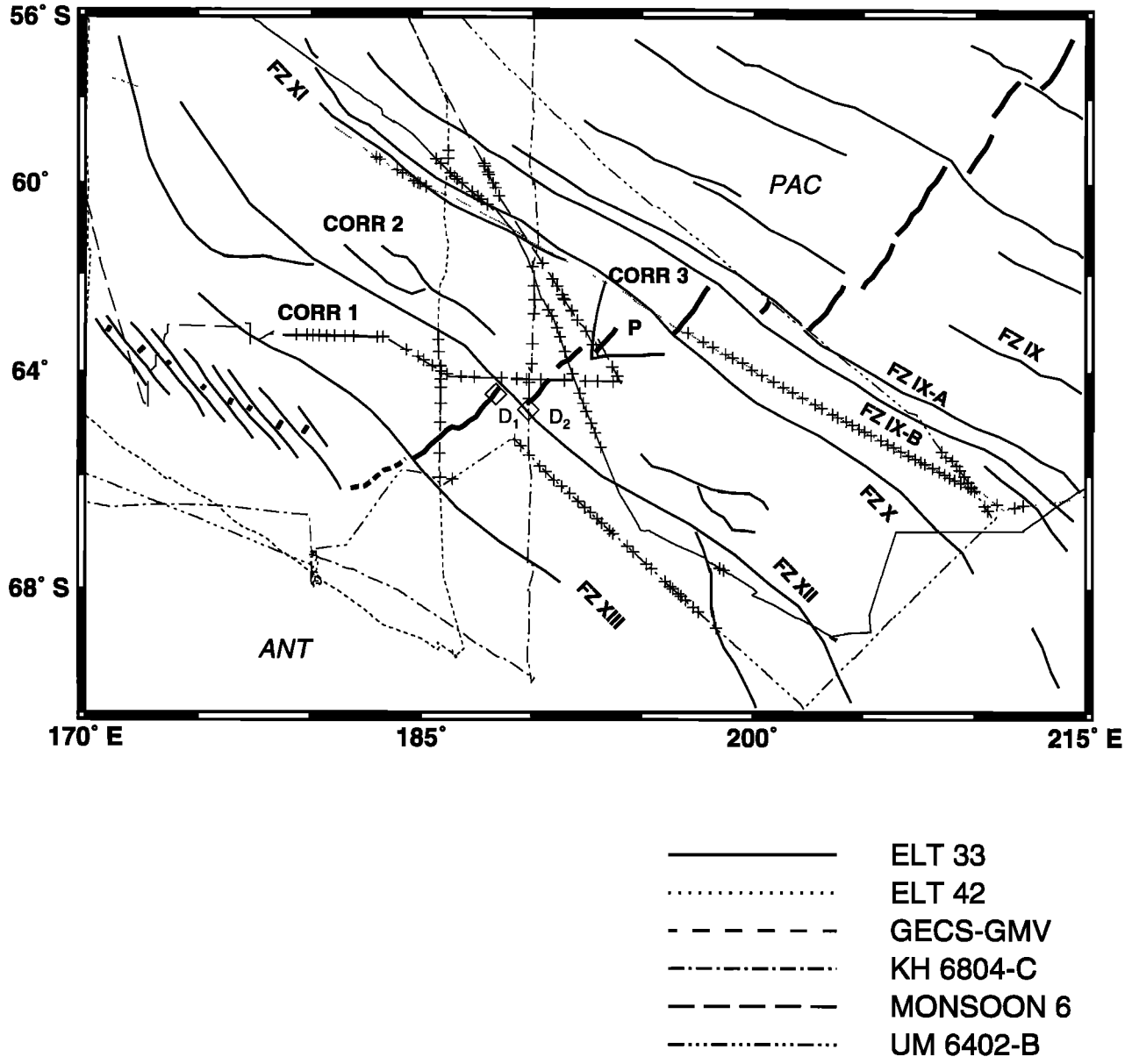

Figure 2. Tectonic features of study area. Heavy lines denote the ridge axis (dashed where uncertain), medium lines are fracture zones (FZ) and pseudofaults (P), thin lines are ship tracks, and pluses are magnetic anomaly locations. Diamonds mark the locations of dredge hauls D_1 and D_2 of *Ferguson et al.* [1992]. Spreading corridor 1 lies to the southwest of FZ XII, and corridors 2 and 3 lie to the northeast. The small-offset ridge/transform system lies to the west of 182°E, and the Y-shaped traces in the gravity field are located in corridor 2.

the gravity field (and seafloor) that are roughly symmetric about the spreading ridge [*Marks and McAdoo*, 1991]. Large fracture zones, which are delineated by sinuous gravity lows, and the spreading ridge, which is associated with a gravity anomaly high, are also evident (these features are outlined in Figure 2). In this study we focus on three segments of spreading ridge that lie between 185°–190°E (corridor 1) and 190°–198°E (corridors 2 and 3). Spreading rates for corridors 1 and 2 have been 63–66 mm/yr (full rate) since about anomaly 2ay time (2.5 Ma on the Decade of North American Geology (DNAG) timescale [*Berggren et al.*, 1985]), as determined from shipboard magnetic data discussed below and shown in Figures 3 and 4.

Morphology and Depth-Age Relationships

It can clearly be inferred from the gravity anomalies that the ridge segments adjacent to FZ XII display distinctly different ridge morphologies: the ridge segment southwest of FZ XII is characterized by a gravity low (a prominent rift valley), while the ridge segments northeast of FZ XII have an axial gravity high (a bathymetric high). Ship bathymetry confirms the presence of a ~400-m axial valley (Figure 3c), and a ~500-m axial high (Figure 3a). This abrupt transition in gravity signature was noted by *Small and Sandwell* [1992], who suggested it may indicate there is an abrupt change of axial structure within the range of intermediate spreading

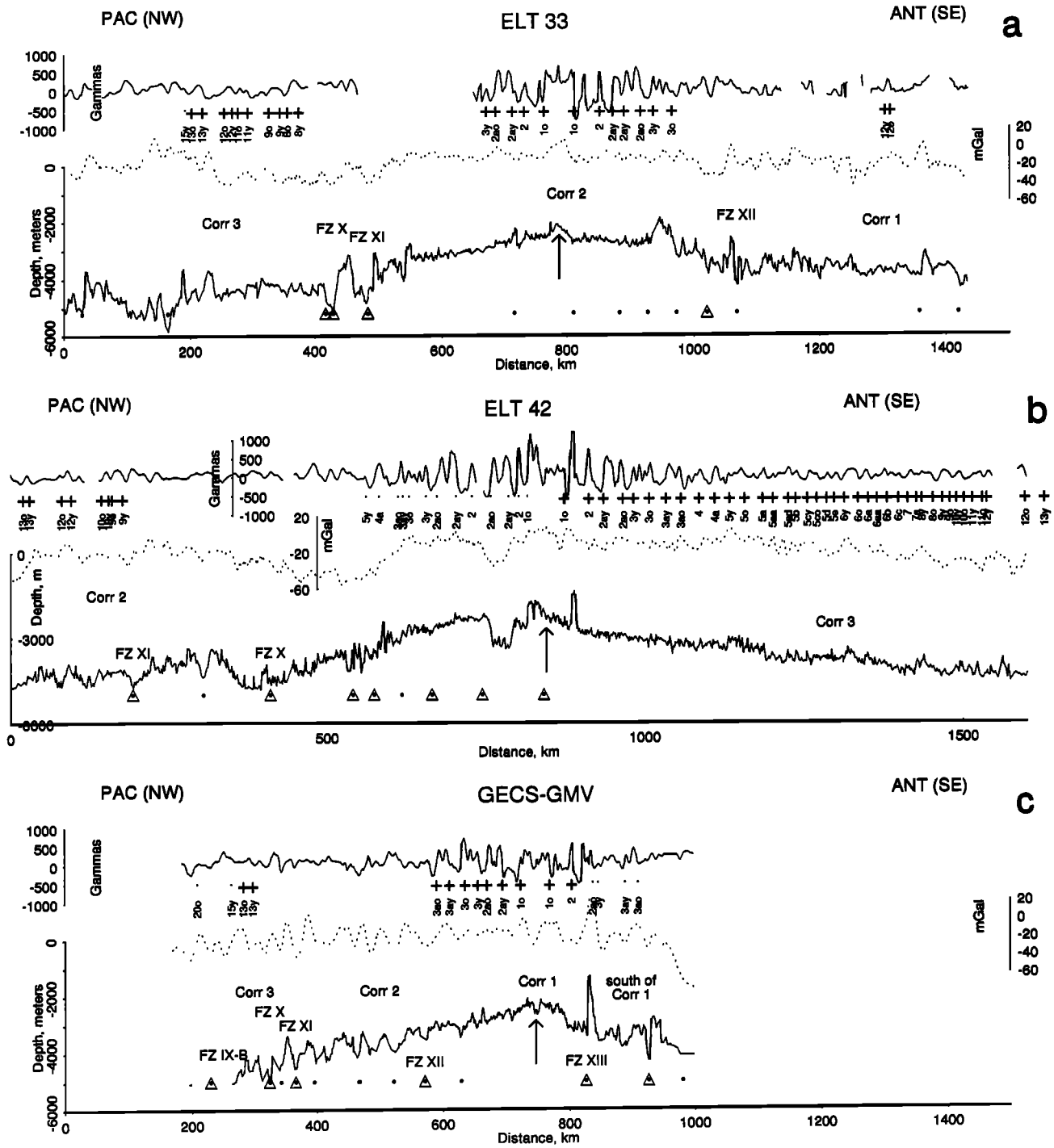

Figure 3. Profiles of bathymetry, total field magnetic anomaly, and satellite gravity for ship tracks shown in Plate 1. The profiles have been projected parallel to an azimuth of 135° (or 315°) (approximately perpendicular to the ridge crest) and run NW to SE (Pacific plate on the left, Antarctic plate on the right). Profiles are aligned along the ridge crest position (arrow) inferred from magnetic isochron and gravity data. Annotated pluses below magnetic anomaly profiles indicate magnetic anomaly picks used in our depth-age calculations. Annotated dots indicate anomalies that were not used in calculating the subsidence rates, either because of their proximity to fracture zones or because they do not lie within the spreading corridors studied here. Dots and triangles below bathymetry profiles indicate fracture zones or topographic anomalies. "P" on Monsoon 6 profile (part A) indicates pseudofaults. Because these profiles cross fracture zones and other offsets, spreading rates measured from this figure must be from carefully selected portions of track, otherwise they may not necessarily represent the actual half rate of plate motion.

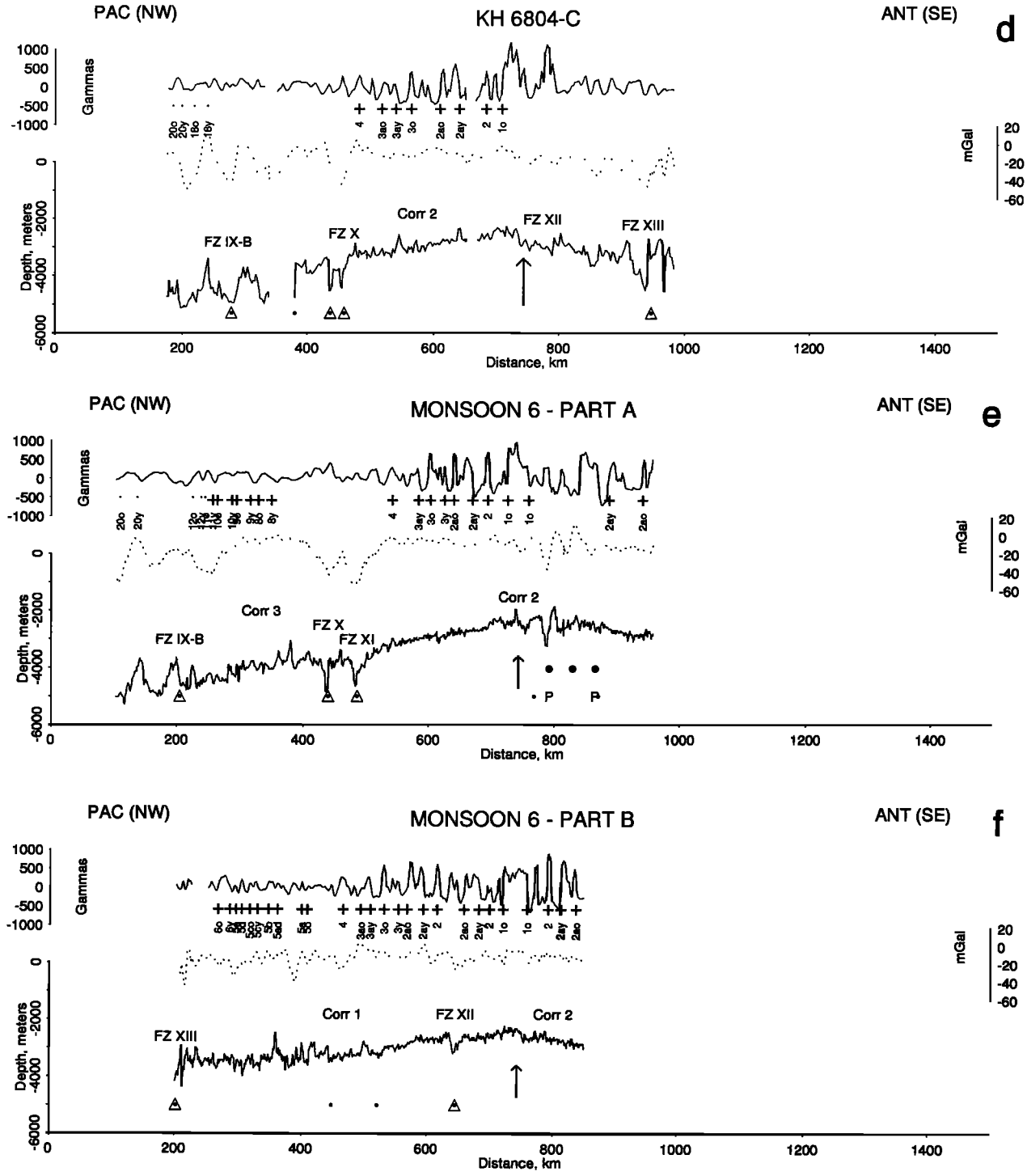

Figure 3. (continued)

rates, instead of a smooth one. The rift valley and axial highs displayed by the ridge segments are not generally characteristic of medium rate spreading ridges such as the Pacific-Antarctic ridge, and the abrupt transition of axial morphology is also not expected of adjacent ridge segments that are spreading at virtually the same rate. The decrease in spreading rate between corridors 1 and 2 (66 to 63 mm/yr if the DNAG timescale is used) appears to be small and gradual, consistent with plate motions on a sphere; it seems unlikely to explain the abrupt morphologic transition across FZ XII.

Although ship track data are sparse in the southern ocean, there are, fortunately, six cruises that traversed the three spreading corridors in our study area (Plate 1) and collected magnetic and bathymetry (or two-way travel time) data pertinent to our depth-age analysis (ship coverage was not adequate enough to enlarge the study area beyond these three corridors). Plotting magnetic data along these ship tracks on the high-resolution Geosat gravity field has enabled us to accurately locate the magnetic anomalies with respect to the spreading corridors. Also, we can now deci-

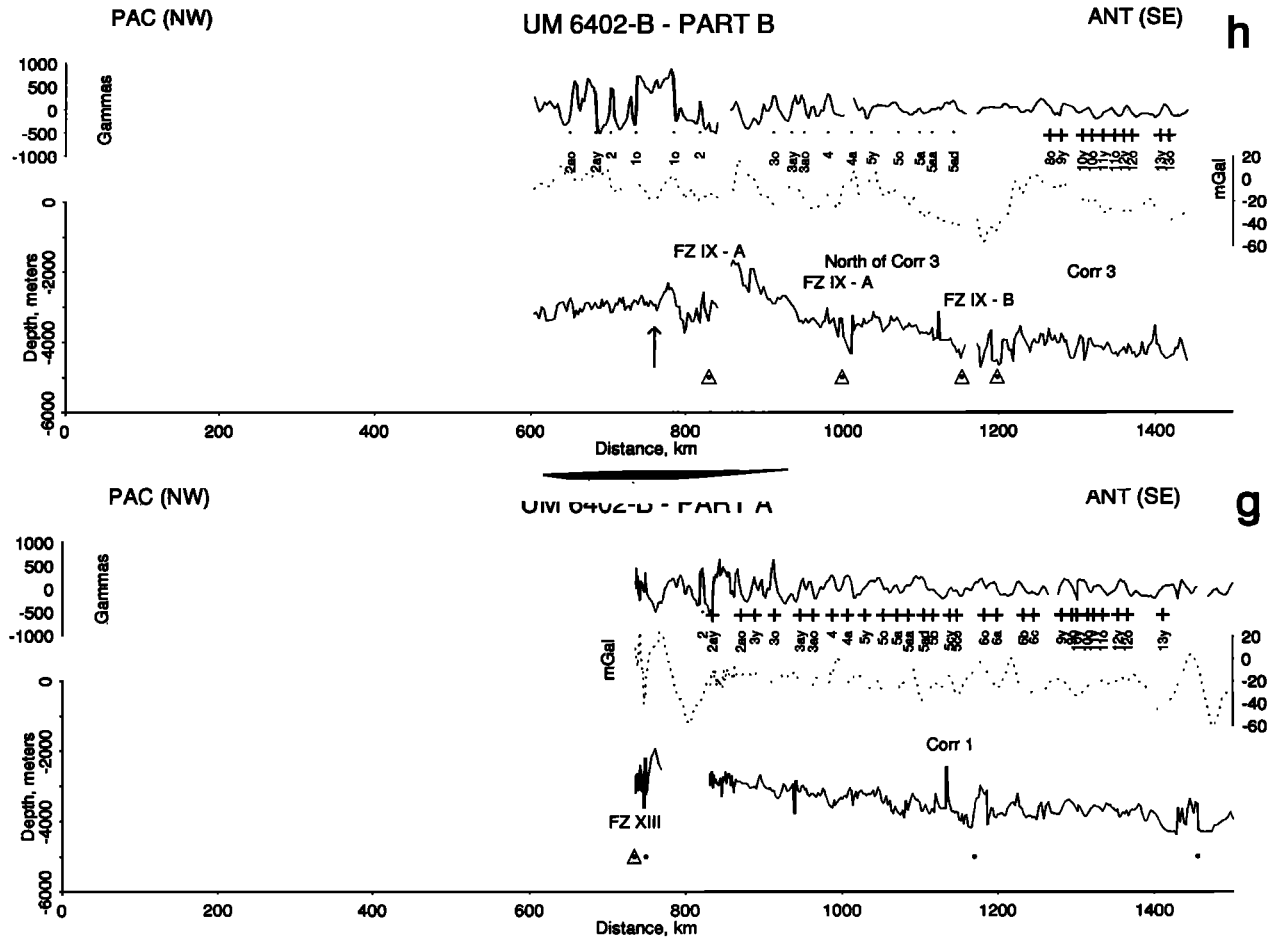

Figure 3. (continued)

pher the ship magnetic and bathymetric data in light of the seafloor tectonics inferred from the Geosat gravity.

As part of a more regional study (J. M. Stock et al., manuscript in preparation, 1993), the relevant magnetic anomalies were identified from the ship track data (Figure 3). From these, a total of 59 magnetic picks were compiled for corridor 1 and 122 for corridors 2 and 3 combined. The locations of these identifications are plotted on the Geosat gravity anomalies in Plate 1. Ages were assigned to the magnetic anomalies using the DNAG timescale [*Berggren et al.*, 1985]; all the magnetic anomalies selected were <36 Ma. Portions of ship tracks Eltanin 42 (Figure 3b), UM6402-B (Figure 3g), GECS-GMV (Figure 3c), and ELT 33 (Figure 3a) are plotted above a synthetic magnetic anomaly profile in Figure 4. The average spreading rates from the present back to the old edge of anomaly 3a (anomaly 3ao) are 58–66 mm/yr if the DNAG timescale is used and 54–61 mm/yr if the timescale of *Cande and Kent* [1992] is used. (This difference arises because of the different ages assigned by these authors to anomaly 3ao: 5.89 Ma and 6.376 Ma, respectively.) Regardless of the timescale chosen, the synthetic magnetic anomalies were computed using anomaly spacings determined from the best fit plate reconstructions for this region (J. M. Stock et al., manuscript in preparation, 1993). These ship magnetic observations demonstrate good agreement with the predicted anomaly spacings, as well as the small decrease in spreading rate from northeast to southwest due to plate motions on a sphere.

Next, we found the depth of seafloor associated with the age determinations. In order to obtain a representative depth, and not one unduly influenced by local short-wavelength topographic features such as seamounts, we applied a Gaussian filter to smooth the ship track bathymetry data. Topographic features less than ~20 km in wavelength were suppressed by the smoothing function. All the smoothed bathymetry values within 10 km of the location of the seafloor age determinations were then averaged, to yield the corresponding seafloor depths. Because sediment cover is thin (<1 km) over the young seafloor in our study area [*Houtz et al.*, 1973], corrections to the seafloor depths for sediment loading were unnecessary.

In order to determine the depth-age relationships for the spreading corridors, we plotted the seafloor depth against the square root of age and calculated the linear relationship (Figure 5). For this analysis we combined data from corridors 2 and 3 because both ridge segments are characterized by an axial high. We used the traditional method of linear regression to fit the best line, where all the uncertainties are assumed to lie in the depths. Although uncertainties are likely to be contained in both ages and depths, the method of functional analysis that accounts for uncertainties in both data yields similar results (within one standard deviation

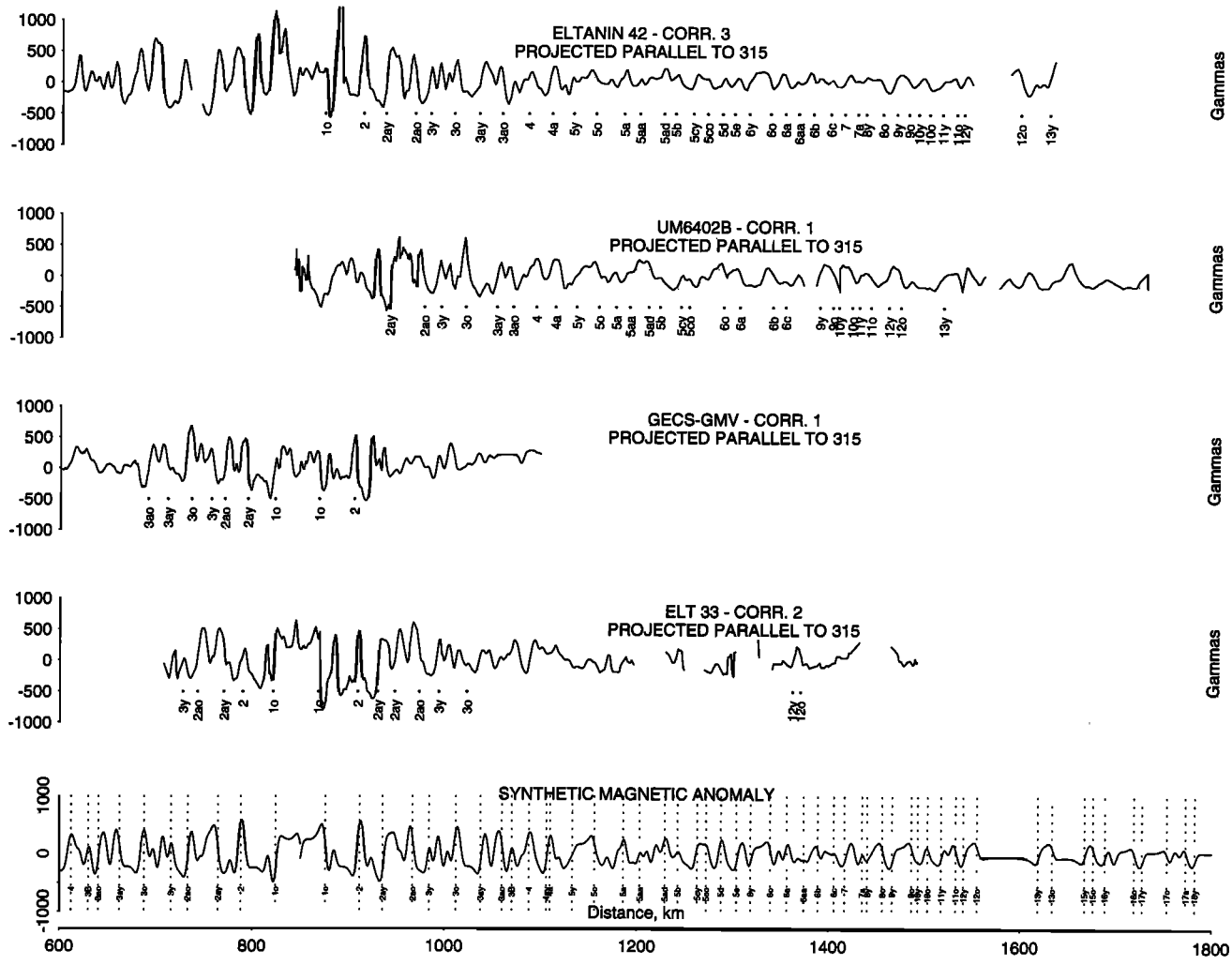

Figure 4. Observed magnetic profiles, and anomaly picks used in this study, from portions of ELT 42, UM6402-B, GECS-GMV, and ELT33 (see Figure 3) plotted above a synthetic magnetic profile computed from best fit plate reconstructions at the location appropriate for the Eltanin 42 line. Spreading rates along the Eltanin 42 line (66–69 mm/yr, corridor 3) are slightly faster than those observed along the UM6402-B and GECS-GMV lines (58–63 mm/yr, corridor 1). This small and gradual decrease in spreading rate from northeast to southwest is due to plate motions on a sphere.

(σ_c) of the traditional line fit), because the scatter about the best line is small.

When all the available data younger than 36 Ma are used, the subsidence constant for the spreading corridor with the rift valley (corridor 1) is 226 ± 13 m/m.y.$^{1/2}$, and the predicted ridge crest depth (at 0 Ma) is 2573 ± 48 m (the ranges are σ_c and σ_{do}). This predicted ridge crest depth agrees well with ship bathymetry observations (Figure 3c). For the spreading corridors with the axial high (corridors 2 and 3), the subsidence constant is 373 ± 6 m/m.y.$^{1/2}$, and the predicted ridge crest depth at 0 Ma is 2195 ± 26 m. Again, the predicted ridge crest depth is corroborated by the ship bathymetry observations (Figure 3a). Because the depths at 0 Ma (plotted as solid circles in Figure 5) were taken from the bottom of the axial valley and the top of the ridge high, they represent the extremes of the axial relief and so were not included in the computation of the line fit.

To test whether the difference in the subsidence rates between the corridors is significant, or if it could be accounted for by fluctuations in the data instead, we used the statistical F test as follows. For corridor 1 and corridors 2 and 3 combined, we computed two linear models to explain the variation of depth with age$^{1/2}$. The first model was the best fit line described above. The second model was a line whose intercept was chosen to best fit the data in the corridor, while being constrained to have a slope equal to the best line for the opposite corridor(s). We obtained the variance of the residuals from each model. The F test can be used to determine whether one model is significantly better than the other by testing the null hypothesis that the two variances are sampled from the same population [*Menke*, 1989]. If there is a good chance (>~10%) that the null hypothesis is true, then there is no significant reason to prefer one model (and hence subsidence rate) over the other.

When we performed this test, we found that the confidence in the null hypothesis was only 10^{-3}; in other words, there is essentially no chance that the two models are equally good, and therefore corridor 1 and corridors 2 and 3 combined have significantly different subsidence rates for ages <36 Ma. The same test was performed using only data

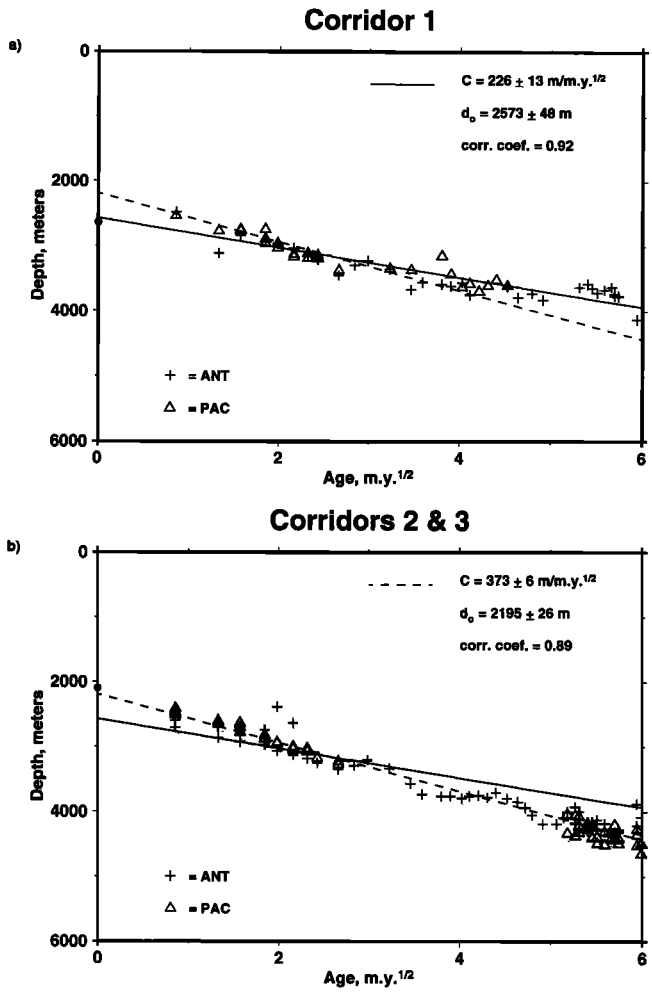

Figure 5. Seafloor depth plotted against age for (a) corridor 1 and (b) corridors 2 and 3 combined. Pluses denote data from the Antarctic plate, triangles data from the Pacific plate, and solid circles the observed axial depths. The solid line is the depth-age relationship computed from observations in corridor 1; the dashed line is from corridors 2 and 3 combined.

younger than 20.45 Ma (anomaly 6o), because there was a large change in plate motion at that time. We found that for ages <20.45 Ma, the null hypothesis has only a 4–8% (virtually no) chance of being true.

Although the exact values of the subsidence constants may be modified by the addition of future data, it seems clear that the spreading corridors adjacent to FZ XII are subsiding at significantly different rates over seafloor younger than 36 Ma. In addition, the spreading corridor with the axial valley is subsiding at an unusually gradual rate, compared to the published depth-age relationships [*Parsons and Sclater*, 1977; *Hayes*, 1988; *Stein and Stein*, 1992]. The implication is that the average thermal regime beneath corridor 1 has been relatively cooler for ages <36 Ma.

Discussion

It is generally accepted that to first order, the morphology of ridges depends on the spreading rate, and the depth of the ocean floor depends on its age. So along a divergent plate boundary that demonstrates no abrupt changes in spreading rate, one would expect adjacent spreading corridors to display similar ridge morphologies and depth-age relationships. However, increasing evidence suggests that spreading ridges may exhibit laterally abrupt morphological and subsidence variations without a change in spreading rate [*Hayes*, 1988; *Cochran*, 1986; *Marks et al.*, 1990; *Small and Sandwell*, 1992]; this region is one such example. There must be a second-order process(es) here that dominates over the first-order ones.

Chen and Morgan [1990] developed models of mid-ocean ridges that produce the observed first-order variations of ridge axis morphology with spreading rate. However, more importantly, they suggest that small changes in crustal thickness and mantle temperatures can have a large effect on the ridge morphology of slow and intermediate spreading ridges. As an example, they suggested that the slow spreading Mid-Atlantic Ridge south of the Iceland hotspot displays the ridge characteristics of a fast spreading ridge because of the inferred elevated mantle temperatures and thicker crust there. They also demonstrated how cooler mantle temperatures can produce a more pronounced axial valley at an intermediate rate spreading ridge.

Likewise, variations in mantle temperature can affect the subsidence constant and hence the depth-age relationship. Cooler mantle temperatures reduce the subsidence constant, whereas hotter temperatures increase it. Both *Cochran* [1986] and *Hayes* [1988] suggested that temperature anomalies as small as 100°C can influence the rate at which the seafloor subsides as it moves away from the ridge. We calculate that average mantle temperatures that are cooler by about 300°C accompanied by a slight mantle density increase (~0.03 g/cm^3) can account for the unusually small subsidence constant of corridor 1 for the past 36 m.y. The subsidence constant from corridors 2 and 3 (373 ± 6 m/m.y.$^{1/2}$), however, is in good agreement with the global average of 365 m/m.y.$^{1/2}$ determined by *Stein and Stein* [1992] (for seafloor younger than 20 Ma) and with 350 m/m.y.$^{1/2}$ found by *Parsons and Sclater* [1977]. Yet the axial high there suggests that the mantle temperatures may be anomalously hot beneath these segments of the spreading ridge.

During the recent detailed ship survey of FZ XII [*Cande et al.*, 1992; *Haxby et al.*, 1992], two basalt samples were collected on the ridge segments adjacent to the fracture zone [*Ferguson et al.*, 1992]. The locations of these samples, D_1 and D_2, are plotted on Figure 2. Geochemical analysis of these basalts suggest that D_1 (in corridor 1) was produced by a smaller extent of melting than D_2 [*Ferguson et al.*, 1992]. Cooler mantle temperatures in corridor 1 are implied by small amounts of melting [*Klein and Langmuir*, 1987].

So a small variation in the temperature of the asthenosphere beneath the Pacific-Antarctic ridge may influence the first-order effect of intermediate spreading rate enough to produce the observed axial rift and axial high and possibly also the different subsidence constants. The implication is that the ridge segments with the axial high overlie relatively hotter asthenosphere than does the ridge segment with the axial rift. We are not certain what would produce a thermal anomaly here, nor how long it might have been present, but we can gain some insight into the possible source by considering the tectonic development of the region in light of our observations.

From at least 35 Ma to ~20 Ma, this part of the Pacific-

Antarctic ridge was spreading at a slower rate (~31 mm/yr), and since ~20 Ma the spreading rate increased to an intermediate rate (J. M. Stock et al., manuscript in preparation, 1993). The most recent major change in spreading rate (to 60–65 mm/yr) occurred around the time that the pole of rotation changed enough to pull open the large fracture zone that originally connected the Southeast Indian ridge to the southernmost segment of the Pacific-Antarctic ridge (~4.7 Ma), initiating a series of short ridge segments offset by small transform faults in this region [*Marks et al.*, 1991a]. We suggest that owing to this increase in the spreading rate, more material was needed for accretion at the ridge axis. The flow along this part of the Pacific-Antarctic ridge appears to be coming from the northeast, where there may be hotspots (such as the Louisville hotspot) or a hot region. It is possible that the ridge segment with the axial valley (corridor 1) may be starved for accretionary materials because the along-axis flow has not yet reached that spreading corridor. Furthermore, if the ridge morphology was typical of slower spreading ridges, then, in the past, ridge segments farther north along the Pacific-Antarctic boundary may also have been characterized by rough topography and an axial valley. So, the ridge axis in corridor 1 may be a vestige of the former axial morphology that has not yet received an adequate supply of hot asthenospheric flow from the northeast to alter its morphologic characteristics. A supply of along-axis flow that diminishes toward the southwest is suggested in the gravity map (Plate 1). The gravity anomaly high along the ridge in the northeast is more pronounced (indicating a more prominent axial high); it becomes gradually more subdued to the southwest until the ridge axis changes from a small axial high to an axial valley across FZ XII.

The features we observe on the Pacific-Antarctic ridge are not unique; there is another spreading ridge with similar, but more pronounced, characteristics. The Australian-Antarctic discordance (AAD) is the portion of the Southeast Indian ridge (SEIR) between 120° and 128°E (see Figure 1). The SEIR both in and around the discordance zone is spreading at an intermediate rate (75 mm/yr full rate). Even so, the ridge morphology and subsidence rates change significantly across the transform fault that bounds the AAD on the east. Within the AAD, the ridge is characterized by a well-defined axial valley and high relief, while the spreading segment to the east displays subdued relief and an axial high. *Cochran* [1986] determined that outside the discordance, the ridge crest depths and subsidence constants are similar to the global average (except for the northern flank east of the AAD which is subsiding at a high rate), while *Hayes* [1988] found that within the AAD the ridge crest is too deep (>1 km deeper than expected) and that the subsidence constant is small (~312 m/m.y.$^{1/2}$). These variations in ridge morphology and subsidence constants are similar to those observed over the Pacific-Antarctic ridge: the spreading corridor with the rift valley and deeper-than-normal ridge crest is subsiding at an unusually gradual rate, and it is adjacent to a one with an axial high (on an intermediate rate spreading ridge).

It has been proposed that the Australian-Antarctic discordance is underlain by cool or depleted upper mantle [*Weissel and Hayes*, 1974; *Forsyth et al.*, 1987] that may tend to be more viscous, so that some of the materials needed for accretion at the plate boundary are more easily supplied by along-axis flow. Westward directed flow from hotspots to the east may be channeled down the ridge axis into the AAD [*Marks et al.*, 1990]. As with the Pacific-Antarctic ridge, the axial high becomes less pronounced towards the AAD. Propagating rifts that approach the AAD from the east (and west) may be driven by this along-axis asthenospheric flow [*Hey and Vogt*, 1977]; indeed lavas collected from these propagating rifts are geochemically identical to those collected from propagating rifts associated with hotspots [*Christie et al.*, 1988].

We suggest that along-axis flow, possibly from nearby hotspots or regions of hot upper mantle, may also influence the ridge morphology and depth-age relationships observed over the Pacific-Antarctic ridge, but in a much more subdued way because the thermal anomaly (and source) is smaller. Although the propagating rift on the Pacific-Antarctic ridge axis at 195°E may be driven by southwestward directed asthenospheric flow, it could also have formed in response to the recent change in the pole of rotation that initiated the leaky transform fault. To date, there are no dredges collected from this propagating rift to test this hypothesis. This is clearly a section of the global ridge system that merits further study in order to test and constrain these models.

Summary

We show that present ridge morphology and the depth-age relationships for seafloor younger than 36 Ma are significantly different for adjacent segments of the Pacific-Antarctic ridge. The spreading corridor southwest of FZ XII has a subsidence constant of 226 ± 13 m/m.y., and its ridge crest is characterized by a prominent axial valley. On the other hand, the ridge segments northeast of FZ XII have a subsidence constant of 373 ± 6 m/m.y.$^{1/2}$, and the ridge crest displays an axial high. The subsidence constant for corridor 1 is smaller than *Parson and Sclater*'s [1977] and *Stein and Stein*'s [1992] global standards. The ridge morphologies are not typical of an intermediate rate spreading ridge or of adjacent ridge segments that are spreading at the same rate.

We suggest that a small variation in mantle temperatures beneath the spreading corridors may influence the first-order effects of spreading rate and plate cooling enough to cause the atypical ridge morphology and differences in subsidence constants. There may be a difference of as much as 300°C between the lower-temperature asthenosphere beneath the segment with the axial valley and the higher-temperature asthenosphere beneath the ridge segments with the axial high. If the source of the hotter anomaly beneath corridors 2 and 3 is similar to that proposed for the Australian-Antarctic discordance, then one would expect either a hotspot or a mantle hot region of another origin, to the northeast. When the spreading rate on the Pacific-Antarctic ridge increased since 20 Ma, so did the need for materials for accretion, which may be supplied in part by along-axis asthenospheric flow from the hot sources to the northeast. We speculate that a sufficient supply of hot asthenosphere has not yet reached the ridge segment with the axial valley, leaving it cooler and starved for accretionary materials.

Acknowledgments. We wish to thank Dennis Hayes and an anonymous reviewer and associate editor whose suggestions led to improvements in this manuscript. Discussions with Walter Smith were also helpful. J. Stock's participation was supported by NSF grant EAR-9058217.

References

Berggren, W. A., D. V. Kent, J. J. Flynn, and J. A. van Couvering, Cenozoic geochronology, *Geol. Soc. Am. Bull.*, *96*, 1407–1418, 1985.

Canadian Hydrographic Service, General bathymetric chart of the oceans (GEBCO), scale 1:10,000,000, 5th ed., Ottawa, Ont., 1982.

Cande, S. C., and D. V. Kent, A new geomagnetic polarity time scale for the Late Cretaceous and Cenozoic, *J. Geophys. Res.*, *97*, 13,917–13,952, 1992.

Cande, S. C., E. M. Herron, and B. R. Hall, The early Cenozoic tectonic history of the southeast Pacific, *Earth Planet. Sci. Lett.*, *57*, 63–74, 1982.

Cande, S. C., J. L. LaBrecque, R. L. Larson, W. C. Pitman III, X. Golovchenko, and W. F. Haxby, Magnetic lineations of the world's ocean basins, scale 1:26,950,000 at the equator, Am. Assoc. of Pet. Geol., Tulsa, Okla., 1989.

Cande, S. C., C. A. Raymond, W. F. Haxby, W. B. F. Ryan, S. Tebbens, S. O'Hara, D. Mueller, B. O'Brien, and M. Wilkinson, Preliminary results of a hydrosweep swath bathymetry, magnetics and gravity survey of a Pacific-Antarctic ridge FZ, I, Plate kinematics (abstract), *Eos Trans. AGU*, *73*(16), Spring Meeting suppl., 295–296, 1992.

Chen, Y. C., and W. J. Morgan, A nonlinear rheology model for mid-ocean ridge axis topography, *J. Geophys. Res.*, *95*, 17,583–17,604, 1990.

Christie, D. M., D. Pyle, J.-C. Sempere, J. P. Morgan, and A. Shor, Petrologic and tectonic observations in and adjacent to the Australian-Antarctic Discordance (abstract), *Eos Trans. AGU*, *69*, 1426, 1988.

Cochran, J. R., Variations in subsidence rates along intermediate and fast spreading mid-ocean ridges, *Geophys. J. R. Astron. Soc.*, *87*, 421–454, 1986.

Cochran, J. R., Systematic variation of axial morphology along the Southeast Indian ridge (abstract), *Eos Trans. AGU*, *72*(17), Spring Meeting suppl., 260, 1991.

Ferguson, E. M., E. M. Klein, S. Cande, W. Haxby, C. Raymond, and D. Coleman, Geochemistry of basalts from the Pacific-Antarctic ridge; 64°S, 171°W (abstract), *Eos Trans. AGU*, *73*(43), Fall Meeting suppl., 605, 1992.

Forsyth, D. W., R. L. Ehrenbard, and S. Chapin, Anomalous upper mantle beneath the Australian-Antarctic discordance, *Earth Planet. Sci. Lett.*, *84*, 471–478, 1987.

Haxby, W. F., C. A. Raymond, S. C. Cande, W. B. F. Ryan, S. Tebbens, S. O'Hara, D. Mueller, B. O'Brien, and M. Wilkinson, Preliminary results of a hydrosweep, gravity, and magnetics survey of a Pacific-Antarctic ridge fracture zone, II, Crustal structure (abstract), *Eos Trans. AGU*, *73*(14), Spring Meeting suppl., 278, 1992.

Hayes, D. E., Age-depth relationships and depth anomalies in the southeast Indian Ocean and south Atlantic Ocean, *J. Geophys. Res.*, *93*, 2937–2954, 1988.

Hey, R., and P. Vogt, Spreading center jumps and sub-axial asthenosphere flow near the Galapagos hotspot, *Tectonophysics*, *37*, 41–52, 1977.

Houtz, R. E., M. Ewing, D. E. Hayes, and B. Naini, Sediments, *Antarctic Map Folio Series*, Folio 17, Plate 5, AGS, Washington, D. C., 1973.

Kent, D. V., and F. M. Gradstein, A Cretaceous and Jurassic geochronology, *Geol. Soc. Am. Bull.*, *96*, 1419–1427, 1985.

Klein, E. M., and C. H. Langmuir, Global correlations of oceanic ridge basalt chemistry with axial depth and crustal thickness, *J. Geophys. Res.*, *92*, 8089–8115, 1987.

Lonsdale, P., Tectonic and magmatic ridges in the Eltanin fault system, South Pacific, *Mar. Geophys. Res.*, *8*, 203–242, 1986.

Macdonald, K. C., Mid-ocean ridges: Fine scale tectonic, volcanic and hydrothermal processes within the plate boundary zone, *Annu. Rev. Earth Planet. Sci.*, *10*, 155–190, 1982.

Macdonald, K. C., The crest of the Mid-Atlantic Ridge: Models for crustal generation and tectonics, in *The Geology of North America*, vol. M, *The Western North Atlantic Region*, edited by P. R. Vogt and B. E. Tucholke, pp. 51–68, Geological Society of America, Boulder, Colo., 1986.

Marks, K. M., and D. C. McAdoo, Tectonic development of the Pacific-Antarctic ridge (abstract), *Eos Trans. AGU*, *72*(17), Spring Meeting suppl., 266, 1991.

Marks, K. M., P. R. Vogt, and S. A. Hall, Residual depth anomalies and the origin of the Australian-Antarctic discordance zone, *J. Geophys. Res.*, *95*, 17,325–17,337, 1990.

Marks, K. M., D. C. McAdoo, and D. T. Sandwell, Geosat GM data reveal new details of ocean floor, *Eos Trans. AGU*, *72*, 145–149, 1991a.

Marks, K. M., D. T. Sandwell, P. R. Vogt, and S. A. Hall, Mantle downwelling beneath the Australian-Antarctic discordance zone: Evidence from geoid height versus topography, *Earth Planet. Sci. Lett.*, *103*, 325–338, 1991b.

Marks, K. M., D. C. McAdoo, and W. H. F. Smith, Mapping the Southwest Indian ridge with Geosat, *Eos Trans. AGU*, *74*, 81–86, 1993a.

Marks, K. M., D. C. McAdoo, and W. H. F. Smith, Geosat gravity anomaly grid south of 30°S, in Global relief data on CD-ROM, *93-MGG-01*, Natl. Geophys. Data Cent., NOAA, Boulder, Colo., March 1993b.

Marty, J. C., and A. Cazenave, Regional variations in subsidence rate of oceanic plates: A global analysis, *Earth Planet. Sci. Lett.*, *94*, 301–315, 1989.

Mayes, C. L., L. A. Lawver, and D. T. Sandwell, Tectonic history and new isochron chart of the South Pacific, *J. Geophys. Res.*, *95*, 8543–8567, 1990.

McAdoo, D. C., and K. M. Marks, Gravity fields of the southern ocean from Geosat data, *J. Geophys. Res.*, *97*, 3247–3260, 1992.

McKenzie, D. P., Some remarks on heat flow and gravity anomalies, *J. Geophys. Res.*, *72*, 6261–6273, 1967.

Menke, W., *Geophysical Data Analysis: Discrete Inverse Theory*, 289 pp., Academic, San Diego, Calif., 1989.

Molnar, P., T. Atwater, J. Mammerickx, and S. M. Smith, Magnetic anomalies, bathymetry and the tectonic evolution of the South Pacific since the Late Cretaceous, *Geophys. J. R. Astron. Soc.*, *40*, 383–420, 1975.

Parsons, B., and J. G. Sclater, An analysis of the variation of ocean floor bathymetry and heat flow with age, *J. Geophys. Res.*, *82*, 803–827, 1977.

Small, C., and D. T. Sandwell, An analysis of ridge axis gravity roughness and spreading rate, *J. Geophys. Res.*, *97*, 3235–3245, 1992.

Stein, C., and S. Stein, A model for the global variation in oceanic depth and heat flow with lithospheric age, *Nature*, *359*, 123–129, 1992.

Turcotte, D. L., and E. R. Oxburgh, Convection in a mantle with variable physical properties, *J. Geophys. Res.*, *74*, 1458–1474, 1969.

Turcotte, D. L., and G. Schubert, *Geodynamics Applications of Continuum Physics to Geological Problems*, 450 pp., John Wiley, New York, 1982.

Weissel, J. K., and D. E. Hayes, The Australian-Antarctic Discordance: New results and implications, *J. Geophys. Res.*, *79*, 2579–2587, 1974.

K. M. Marks, Geosciences Laboratory, Ocean and Earth Sciences, NOS, NOAA, N/OES12, 1305 East-West Highway, Silver Spring, MD 20910.

J. M. Stock, Seismological Laboratory, MS 252-21, California Institute of Technology, Pasadena, CA 91125.

(Received July 23, 1992; revised August 11, 1993;
accepted September 28, 1993.)